

Soft X-ray components in the hard state of accreting black holes

Caroline D’Angelo¹*, Dimitrios Giannios¹, Cornelis Dullemond², and Henk Spruit¹

¹ Max-Planck-Institut für Astrophysik, Karl-Schwarzschild-Str. 1, 85741 Garching, Germany

² Max-Planck-Institut für Astronomie, Königstuhl 17, 69177 Heidelberg, Germany

Received / Accepted

Abstract. Recent observations of two black hole candidates (GX 339-4 and J1753.5-0127) in the low-hard state ($L_X/L_{\text{Edd}} \approx 0.003 - 0.05$) suggest the presence of a cool accretion disk very close to the innermost stable orbit of the black hole. This runs counter to models of the low-hard state in which the cool disk is truncated at a much larger radius. We study the interaction between a moderately truncated disk and a hot inner flow. Ion-bombardment heats the surface of the disk in the overlap region between a two-temperature advection-dominated accretion flow and a standard accretion disk, producing a hot ($kT_e \approx 70\text{keV}$) layer on the surface of the cool disk. The hard X-ray flux from this layer heats the inner parts of the underlying cool disk, producing a soft X-ray excess. Together with interstellar absorption these effects mimic the thermal spectrum from a disk extending to the last stable orbit. The results show that soft excesses in the low-hard state are a natural feature of truncated disk models.

Key words. Accretion, accretion disks - Radiation mechanism: general - Black hole physics

1. Introduction

The geometry of the low-luminosity (“low-hard”) state of Galactic Black Hole Candidates (GBHC), in which the spectrum is dominated by a power law X-ray flux extending to high energies, has been an open question for several decades. While it is generally believed that the power law spectrum is formed by inverse Compton scattering, there is no consensus about the geometry of the flow, source of seed photons or energy distribution for the Comptonizing electrons.

Broadly speaking, there are two classes of model to explain the spectrum in the low-hard state. The first is the “corona” model, in which the disk remains untruncated or nearly untruncated at luminosities $L_X \approx 10^{-3}L_{\text{Edd}}$. The hard power law spectrum comes from a hot and patchy corona (perhaps powered by magnetic flares (di Matteo 1998; Beloborodov 1999; Merloni & Fabian 2001)) on top of the disk, while the surrounding region is bombarded with high energy photons, producing the observed reflection and Fe-K fluorescence components. In the alternate, “truncated disk” model the thin disk is truncated at some distance from the black hole and the inner region is filled with a hot, radiatively-inefficient flow, which produces the hard spectrum. The reflection spectrum and Fe-K fluorescence is then produced by the interaction of the hard X-rays with the inner part of the truncated disk, or in some cool outflow moving away from the disk. For a recent discussion of the low-hard state see sect. 4 of Done et al. (2007).

In theory, the presence or absence of a cool disk should be confirmable through direct detection of a soft X-ray blackbody

component at low energies. In practice however, this is made difficult by the fact that at low accretion rates the temperature of even an untruncated disk will drop from about 1-2keV in the high soft state to $\sim 0.1-0.3\text{keV}$, which puts it out of the range of most X-ray detectors. Additionally, the effects of interstellar absorption become very strong at around 0.1keV, so that detecting a soft excess and accurately measuring its parameters will depend somewhat on how accurately the interstellar absorption can be determined.

Even with these challenges, a soft excess in the low-hard state has previously been reported in several sources. The first was Cyg X-1 (Balucinska-Church et al. 1995; Di Salvo et al. 2001), although its association with an accretion disk is complicated by the fact that Cyg X-1 is a high mass X-ray binary accreting from a wind. This question was also the focus of two recent papers, Miller et al. (2006a,b), in which the authors studied long-exposure *XMM-Newton* spectra of two different GBHCs, SWIFT J1753.5-0127 and GX 339-4, at low luminosities ($L_X/L_{\text{Edd}} \sim 0.003 - 0.05$). Soft excesses at similar luminosities in these two sources have also been reported in Ramadevi & Seetha (2007) (J1753.5-0127) and Tomsick et al. (2008) (GX 339-4). Since these two observations, there have also been observations of soft excesses in several other sources. Rykoff et al. (2007) made several observations of the soft component of XTE J1817-330 with *Swift* during the outburst decline of that source down to a luminosity of $L_X/L_{\text{Edd}} \sim 0.001$, while a soft component in GRO J1655-40 has been reported by both Brocksopp et al. (2006) and Takahashi et al. (2008) using different telescopes.

* dangelo@mpa-garching.mpg.de

To interpret the soft excesses in SWIFT J1753.5-0127 and GX 339-4, Miller et al. (2006a,b) fit the data with a several *XSPEC* models, trying various black-body disk models and simple hard X-ray components (both a power law and various Comptonization models). In GX 339-4 a broad Fe-K line was also observed and fit with a relativistically broadened reflection model. Using blackbody models for a standard accreting disk, the authors found disks with maximum temperatures of $kT \sim 0.2\text{-}0.4$ keV, and inner radii consistent with the innermost stable circular orbit of a black hole.

At the inferred low accretion rates in the hard state, a disk extending to the last stable orbit would produce a soft X-ray component with peak close to the cutoff due to interstellar absorption. Unless an accurate independent measure of the interstellar absorption column is available, spectral fitting procedures cannot reliably distinguish between a thermal peak at $kT = 0.3$ keV with one interstellar absorption column and a cooler component with a lower energy component cutoff by a slightly higher interstellar absorption column.

For energetic reasons the hard X-ray component which dominates the luminosity in the hard state must originate near the black hole, the same region as the proposed cool disk. Some form of interaction of hard X-rays with the cool disk must take place, and this implies that the isolated cool disk models used as ‘components’ in fits to observed spectra are unrealistic. In fact, most models for the hard X-ray component include some prescription for the reprocessing of hard into soft radiation, whether these be truncated disks or extended disk models. As shown by Haardt and Maraschi (1991), such models generically produce a similar energy flux in soft and hard X-rays. A strong soft component is thus a natural consequence in truncated as well as extended disk models for the hard state.

The main difference in a truncated disk model is that the soft flux originates from a larger surface area and consequently has a lower temperature, putting its spectral peak below 0.5 keV. After interstellar absorption the soft component has a peak around 0.5 keV that can be mistaken for an apparent thermal peak with the temperature of a disk near the last stable orbit.

In this paper we examine this with a more quantitative model for truncated disks. At the inner edge of a truncated disk the accretion flow must change in nature from a relatively cool, thin disk into a much hotter, vertically-extended inner flow. There will thus necessarily be some interaction between the two, either through radiation (e.g. Haardt & Maraschi (1991)) or matter exchange (Spruit 1997), or both. Our goal is to determine whether such a model could reproduce the soft spectral components reported by Miller et al. (2006a,b). We will find that disks truncated at 15–20 Schwarzschild radii can in fact produce soft components of the observed strength and shape. An alternative model investigating re-condensation from an ADAF is considered by Taam et al. (2008).

2. Physics of Interaction Region

2.1. Origin of Soft Excesses

Determining the inner radius of an accretion disk from its spectrum relies on (among other things) an accurate understanding

of how luminosity in the disk is produced. In the higher luminosity “high-soft” state, (approximately) blackbody flux from the disk dominates the spectrum. The disk’s inner radius can be inferred, provided the distance and inclination of the source are known, from the assumption that the radiation is produced by internal viscous dissipation in the disk as it accretes, and an assumed ‘color correction’ to the blackbody spectrum.

However, when the spectrum becomes dominated by very hard X-ray and γ -ray radiation, the radial temperature and luminosity profile of the disk will depend on the interaction between the hard radiation and the disk. This is because most of the accretion power is now in the hot gas producing the hard radiation, some of which will interact with the cool disk (as is seen in the reflection spectrum and Fe fluorescence), and may provide a substantial source of heating. This heating of the disk surface converts the hard radiation into a soft component. In the simplest version of this model, Haardt & Maraschi (1991) calculated the energy balance for a hot corona covering a cool disk and found that the flux in the soft and hard components will be roughly equal. This predicts that a substantial soft X-ray component is a universal feature of the hard-state spectrum, whether the disk is truncated or not. Its detectability depends on the sensitivity of detectors in the 0.1-1 keV range, and the interstellar absorption column.

For models in which a cool, truncated accretion disk encircles a very hot inner flow (which cools through inverse Compton scattering), there will necessarily be a region of interaction near the truncation radius, which will heat the inner edge of the disk. This will come either from hard photons bombarding the disk as in the Haardt-Maraschi model, or through matter interaction, with hot protons from the inner flow directly colliding with the cool disk. In both cases previous work has shown that a soft component is produced, but a more detailed model is needed to predict the radiation spectrum. The first case, examining the structure of a thin accretion disk bombarded by hard photons has been studied by for AGN disks Ballantyne et al. (2001) and Nayakshin & Kallman (2001), and more recently for GBHC disks by Ross & Fabian (2007). In this paper we focus on the second case, in which a moderately truncated disk is embedded in a hot, two-temperature advection-dominated accretion flow (ADAF).

2.2. Definition of the model

We begin with the results from a prototype model for ion bombardment on cool disks, initially proposed by Spruit (1997), and extended in Spruit & Deufel (2002), Deufel et al. (2002) and Dullemond & Spruit (2005) (hereafter DS05). In this model a cool disk is embedded in a two-temperature ADAF in which the protons are close to their virial temperature (~ 20 MeV). The protons bombard the disk, and are stopped via Coulomb collisions with the disk’s electrons, thus transferring their energy to the disk. The energy from the protons is sufficient to evaporate the upper layers of the disk into a hot corona with $kT_e \sim 60 - 80$ keV (called the “hot layer” in our nomenclature, although the temperature in this layer is still much cooler than the virial temperature), whose temperature is set by

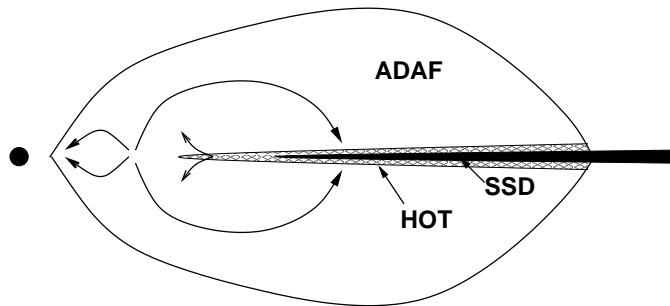


Fig. 1. Schematic structure of a cool disk embedded in an ADAF. Here the ADAF (the transparent outer region) extends over the inner edge of the cool Shakura-Sunyaev disk (SSD), shown by the solid thin disk, bombarding it with high energy protons ($kT_p \sim 20$ MeV). This evaporates the surface of the disk into a ($kT_e \sim 70$ keV) corona, called here the hot layer (HOT LAYER, hatched). The higher viscosity of the hot layer causes it to spill over the inner edge of the SSD where cooling through inverse Compton scattering is no longer efficient (HOT RING), and thermal instability causes the layer to evaporate into the ADAF. The mass transfer is represented by the small arrows.

a balance between heating from the ions and cooling, predominantly through inverse Compton scattering of disk photons. Deufel & Spruit (2000) found that the optical depth of the hot layer is around unity, varying only weakly with irradiating flux and distance from the hole.

The higher viscosity of the hot layer also allows it to spill over inside the inner edge of the cool disk (see fig. 1). Using 1-D simulations, Deufel et al. (2002) suggested that the lack of seed photons in this layer will cause the temperature to rise to about $kT_e \sim 200 - 300$ keV, since cooling from inverse Compton scattering will be much less efficient. Spruit & Deufel (2002) found that this region will become unstable and evaporate into the ADAF. This shows how an ADAF can be maintained inside a truncated cool disk. The key for the whole process is the presence of a component of intermediate temperature (the hot layer). On one hand this component produces a hard, Comptonized spectrum, while on the other its evaporation feeds the ADAF.

DS05 extended this work to examine the radial dependence of the three components of the flow. They set up a model in which the truncation radius of the cool disk is a free parameter, and the three layers are assumed to interact only via the mass transfer processes outlined above. They assumed the cool disk was a standard Shakura-Sunyaev disk (Shakura & Sunyaev 1973), and that the ADAF flow temperature followed the model of Narayan & Yi (1994). They approximated the temperature in the hot layer to be constant, and also assumed a constant temperature for its extension inside the inner edge of the cool disk (which we will call here the “hot ring”)¹. With these assumptions, the radial profiles of the three

¹ The nomenclature we adopt in this paper is slightly different from DS05. They referred to the ADAF as an “ISAF”, or Ion-Supported Accretion Flow, while what we have called the “hot inner ring” they

components can then be determined by solving the equations for mass and angular momentum conservation for a thin disk.

This simplified analysis yields for each component estimates of the mass accretion rate \dot{M}_i , heating rate Q_i (from internal viscous dissipation and ion heating), and surface density Σ_i as a function of radius. For further discussion of the model, see sect. 2 of DS05.² The input parameters for the model are the black hole mass M_{BH} , the magnitude of the α viscosity parameter (Shakura & Sunyaev 1973), and the truncation radius R_{SSD} for the disk. A sketch of the model with its various components is seen in fig. 1. Assuming we know the dominant radiation mechanisms, we can determine the spectrum from the resulting energy distribution for each layer. This is the primary goal of the current work.

2.3. Energy and mass balance

The three components of the model exchange mass and energy. In the steady state assumed here, the sources and sinks balance in each. The topmost layer, the ADAF, loses mass and energy to the hot layer, at rates per unit area of the order $c_{s,i}\rho_i$ and $c_{s,i}w_i$, respectively. Here $c_{s,i}$, ρ_i , and w_i are respectively the thermal speed in the ADAF (i.e. near the virial speed or orbital velocity), the density, and enthalpy. Depending on its radiative efficiency the ADAF could make a substantial contribution to the hard X-ray flux in addition to the flux from the ion-heated hot layers. For our prototype model we ignore this contribution, since Esin et al. (1997) estimate the efficiency of an ADAF to be about $\epsilon \sim \dot{m}\alpha^2 \simeq 1.5 \times 10^{-4}$ (where \dot{m} is the accretion rate scaled in terms of Eddington). If this is the case, the luminosity of the ADAF will scale with \dot{m}^2 , while the energy influx into the cool disk scales as $\rho_i \sim \dot{m}$, (since $T \sim T_{vir}$ in the ADAF), meaning that the ADAF’s indirect contribution to radiation through heating the cool disk will dominate at low luminosities. However, the radiative efficiency of hot inner ring is strongly model dependent, and may be much higher, which would make the spectral contribution of the ADAF important. We discuss this question further in sect. 4.

There is a mass flux by evaporation from the hot layer into the ADAF, as derived in Spruit & Deufel (2002). The energy flux into the ADAF associated with this evaporation can be neglected, since the temperature of the hot layer is low compared with the temperature of the ion flow. The hot layer is heated in similar measure by viscous dissipation and the hot ions it absorbs from the ion flow above ($Q_{visc,w} = 2 \times 10^{16}$ ergs⁻¹cm⁻², and $Q_{i,w} = 7 \times 10^{15}$ ergs⁻¹cm⁻², respectively for the reference model). It is cooled by Compton upscattering of disk photons passing through it, which will produce a hard X-ray spectrum.

There is also a mass flux feeding mass into the hot layer from the cool disk underneath; it is parametrized as in sect. 2.2 of DS05. The cool disk is heated in three ways: by internal viscous dissipation, by reprocessing of hard (Comptonized) X-

term the “hot layer”, and our “hot surface layer” is in that paper referred to as the “warm layer”.

² We note that in that work the numerical factor of equation (2) is incorrect, it should be 2.64×10^8 , and equation (3) should be the same as equation (16) in Spruit & Deufel (2002).

rays from the hot layer above, and by the (small) number of hot ions from the ADAF that pass through the hot layer.

The reprocessing of the hard X-rays is further divided into a fraction a that is *reflected*, and a fraction $(1-a)$ that is absorbed and assumed to thermalize completely. The reflection process and the spectrum resulting from it are based on results from the literature; this is described in sect. 2.4.2. The spectrum of the cool disk feeding photons to the Comptonization process in the hot layer thus consists of a blackbody component plus a reflection spectrum.

The surface temperature of the cool disk, assumed to be close to its effective temperature, is given by

$$\sigma_B T_{eff}^4 = Q_{c,visc} + (1-a)F_h^- + f_c Q_i, \quad (1)$$

where $Q_{c,visc}$ is the viscous heating rate of the cool disk c , a its X-ray reflection albedo, F_h^- the flux of downward directed X-ray photons from the hot layer h , and $f_c Q_i$ the fraction f_c of the energy flux Q_i in hot ions that make it through the hot layer and are absorbed instead in the cool disk. The albedo a of the disk depends on how ionized the disk is, which we discuss more in sec. 2.4.2.

Compton upscattering of the soft flux from the cool disk determines the detailed shape of the spectrum emerging from the hot layer. In addition there is an X-ray component from the ‘hot ring’ interior to the inner edge of the cool disk. Since it receives fewer of the soft photons and hence is hotter, it adds a harder component to the spectrum.

These ingredients are the same as in DS05, except that the reflection process is included more realistically, and the Comptonization of soft photons is treated in detail with the Monte Carlo code of Giannios (see sec. 3) so a realistic X-ray spectrum is obtained.

2.4. Reference model

We illustrate the model first with representative parameter values for a black hole binary. In sects 3.1 and 3.2 the parameters are adjusted for application to observations of specific objects.

We take $M_{BH} = 10M_\odot$ for the mass, $R_{in} = 20R_S$ for the truncation radius (where $R_S = 2GM/c^2$ is the Schwarzschild radius). A typical if somewhat large viscosity parameter $\alpha = 0.2$ is used for all accretion components. The flow model of DS05 yields an accretion rate of $\dot{M} = 3.1 \times 10^{16}$ g/s for these parameter values. In terms of the Eddington accretion rate (defined here with an assumed bolometric efficiency of 10%) this translates to $\dot{M} = 2.2 \times 10^{-3} \dot{M}_{Edd}$ ³, and bolometric luminosity is $L_X = 4.2 \times 10^{-4} L_{Edd}$, which is significantly lower than observed luminosities for the low/hard state. We discuss this discrepancy and possible solution further in sects 3 and 4.

In fig. 2 we show the temperature profile of the cool disk component of this reference model. The dashed line shows the temperature profile that would result if only the viscous dissipation in the cool disk were included. The cool disk is completely

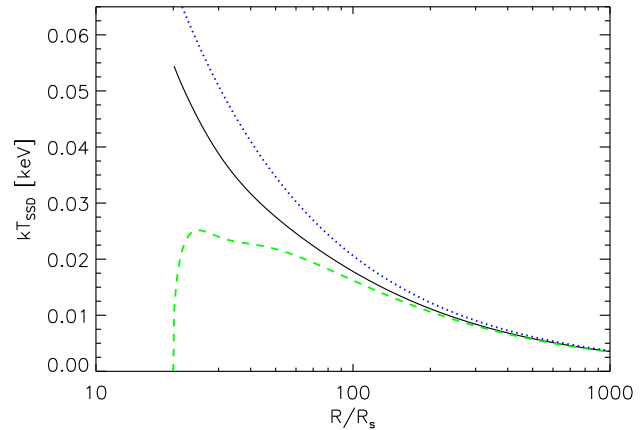


Fig. 2. Effect of ion-bombardment on the surface temperature of a cool (SSD) disk with inner edge at $20R_S$ (for the other model parameters see text). Black solid line: radial temperature profile when disk heating is considered. Green dashed line: radial temperature profile in disk without considering heating from hot layer. Blue dotted line: radial temperature profile for an untruncated disk at the same accretion rate.

evaporated into the hot layer before the inner edge of the accretion disk, hence its surface density drops to zero at the inner edge of the disk in the same way as for a standard cool disk accreting on a slowly rotating object (the standard ‘zero-torque inner boundary condition’). If there were viscous coupling between the inner edge of the disk and the hot ring, however, the resulting temperatures near the inner edge would be higher than in our current model. This would result in a stronger soft component, whose contribution would remain observable for larger truncation radii than we have considered here. The solid line shows the effect when heating from the hot layer is included. As can be seen in the figure, the effect of heating extends to large radii. The dotted line shows the temperature profile for an standard untruncated disk for the same accretion rate.

We can also compute the bolometric radiative efficiency for the model, assuming that the hot layer and inner ring radiate efficiently. For our reference model with a disk truncated at $20R_S$, we find a radiative efficiency (the ratio of the total luminosity to the accreting rest-mass energy flux) of about 4%. In comparison, the radiative efficiency of a disk truncated at $20R_S$ alone is about 1%, which demonstrates that the ion-bombardment process can significantly increase the radiative efficiency.

2.4.1. Cool disk emission

We begin by estimating the spectrum of the radiation produced by the thin disk, i.e. the seed photons of the Comptonization in the hot layer. At large effective optical depths in the disk the radiation field is a blackbody. The flux emerging from the photosphere of the disk is reduced, however, by Thomson scattering, resulting in a ‘modified blackbody’, a spectrum with same temperature but reduced flux. In the literature, it is often described equivalently by a ‘color correction’ factor f_{col} ,

³ In DS05 a plotting error resulted in the mass accretion rates in all figures being overstated by a factor of 100 with respect to the Eddington rate.

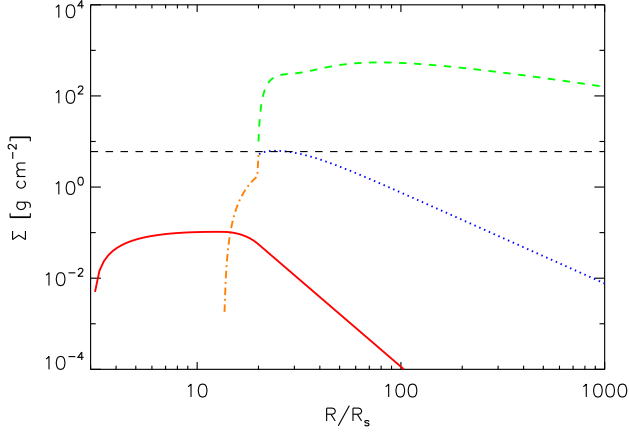


Fig. 3. Surface density (Σ) profile for reference model, where $M_{BH} = 10M_{\odot}$, $\alpha = 0.2$ and $R_{ssd} = 20R_s$. Green dashed line: Shakura-Sunyaev disk. Blue dotted line: Hot layer. Orange dash-dotted line: Hot ring. Red solid line: ADAF.

measuring the effect instead as the ratio of color temperature to effective temperature, $T_{col} = f_{col}T_{eff}$. Several papers have done extensive calculations of this spectral hardening in the outer layers of a disk dominated by electron scattering, including Shimura & Takahara (1995), Merloni et al. (2000), and Davis et al. (2005), and concluded that the color-correction is of the order $f_{col} \approx 1.4 - 2$, with the magnitude of correction increasing gradually as the luminosity increases. The approximation of a single parameter across the entire spectrum become less good as the flux decreases.

In a cool disk the (vertically integrated) viscous dissipation Q_{visc} is balanced by radiative loss at its surface,

$$Q_{visc} = \sigma_B T_{eff}^4 = \sigma_B (T_{col}/f_{col})^4. \quad (2)$$

The value for f_{col} will change the determination of the inner disk radius, since the luminosity will be depressed by a factor of f_{col}^{-4} relative to the temperature, so that when color correction is considered, the inner radius of the accretion disk will be increased by a factor f_{col}^2 .

In this work we have the additional complication of the hot surface layer, which will heat the upper layers of the disk substantially and may change the spectral hardening. Ross & Fabian (2007) have estimated the effects of incident hard X-ray radiation on galactic black hole disks, although they focus on systems in which the disk is hotter ($kT \sim 0.35$ keV) than ours and dominates the overall spectrum. However, they do find substantial spectral hardening, and disk temperatures which increase with increasing X-ray flux (fig. 4 of that paper). They also find that the incident radiation can change the ionization structure of the upper layers of the cool disk, so that the shape of the disk spectrum is significantly altered by absorption lines (see their fig. 6).

Since it is beyond the scope of this work to do a similar radiation transfer calculation, we instead choose a single color correction factor, $f_{col} = 1.7$ as a typical value for all our models.

2.4.2. Reflection spectrum

The hard flux incident on the cool disk undergoes reprocessing by electron scattering and atomic processes, giving rise to a series of emission lines (especially the Fe-K fluorescence line) and a Compton reflection hump. In the course of these processes, part of the incident energy flux ends up heating the plasma. Detailed calculations of these processes is beyond the scope here. Instead, we simplify the physics by separating the incident flux into a reflected part and a part that is treated as being absorbed. We treat the absorbed part in the same way as the energy input by viscous dissipation in the disk, i.e. a fraction $(1 - a)$ is added to the left hand side in (2).

The remaining part is treated by a modified version of the XSPEC model “REFLION” described in (Ross & Fabian 2005). This model calculates the reflection spectrum of a power law flux between 0.1-300 keV hitting a constant density AGN disk. We set the lower cutoff of this power law at 0.2 keV, since we expect disk temperatures around 0.1 – 0.2 keV. REFLION calculates the reflection spectrum for a fixed ionization parameter, $\xi \equiv 4\pi F_X n_H^{-1}$, the ratio of the incident flux on the disk to the hydrogen number density. The disk, however, is stratified, so an estimate has to be made of the depth in the disk atmosphere where most of the reprocessing takes place. We assume here that this depth is just the electron scattering photosphere of the cool disk, $\tau_{es} = 1$. By hydrostatic balance, the pressure at this depth is approximately

$$P \approx \frac{g}{\kappa_{es}}, \quad (3)$$

where g is the vertical component of the acceleration of gravity at the height of $\tau_{es} = 1$ above the midplane. Assuming this height is about twice the nominal disk thickness $H = c_s/\Omega_K$, the pressure is $P \approx 2c_s\Omega_K$. Here c_s is the sound speed at the midplane of the disk, which is determined from the heating rate Q_{visc} by a standard thin disk model. To fix the density corresponding to this pressure the temperature has to be determined. We assume for this the effective surface temperature T_{eff} that follows from the viscous heating rate. If F_h^- is the incident X-ray flux from the hot layer, the ionization parameter is then

$$\xi \approx \frac{2\pi F_h^- k T_{eff} \kappa_{es}}{\Omega_K c_s}. \quad (4)$$

The value of ξ varies with distance r from the black hole; an energy-weighted mean is $\xi \approx 10$ erg cm s⁻¹ for the reference model. We use this as a representative value for the reflection calculation instead of an integration over the disk. For this value of ξ , the resulting albedo is low (≈ 0.2), so that most of the hard flux is absorbed and thermalized in the disk. The total reflection and disk spectrum (before being passed through the hot layer), is seen in the red long-dashed line in fig. 4. This is the input spectrum for the Comptonization by the hot layer. Since the optical depth of the hot layer is only around unity, it will also make a significant direct contribution to the output spectrum.

2.4.3. Uncertainties in the reflection spectrum

Through its effect on the gas density, the temperature assumed in the reprocessing region has a direct effect on the ionization parameter and the resulting reflection spectrum. Unfortunately, there is a significant uncertainty in this temperature, since it depends itself on the ionization parameter. At low densities higher in the atmosphere, the ionization parameter is high and the temperature will be close to the Compton temperature of the incident X-ray spectrum. For our reference model, this would be around 3 keV. Deeper in the atmosphere, the ionization parameter would be lower and the temperature closer to equilibrium with the energy density of the radiation field, of the order of the effective temperature of the cool disk. Since the transition between these regimes takes place around the reprocessing layer itself, all depends on details of the radiation physics.

Several groups (Ballantyne et al. 2001; Nayakshin et al. 2000) have calculated the change in the vertical structure of AGN disks as a result of incident hard radiation, and found the upper layers become stratified, with the top being heated to close to the Compton temperature and a sharp transition to the inner layer which radiates at the disk's effective temperature. They find that this stratification will change the disk's reflection properties substantially. Although Ross & Fabian (2007) study a similar situation in galactic black holes, and find no similar stratification, they focus on cases in which the disk dominates the luminosity. For lower disk temperatures stratification could presumably still occur. However, Nayakshin & Kallman (2001) studied the case where a disk was overlaid with a surface corona, and included the effect of its weight on the gas pressure. They found that this was sufficient to prevent stratification.

An additional caveat in using the constant density models of Ross & Fabian (2005) is that they consider AGN disks, which are much cooler and less dense than those in GBHCs. As a result, the reflection spectra do not consider the flux in the disk itself (which can change the ionization state significantly), and the effects from things like three-body recombination, which will become important as the disk densities become higher. Recent work by Ross & Fabian (2007) has examined reflection spectra in GBHCs, although they focus on systems in which the disk dominates the spectrum and is hotter ($kT_e = 0.35$ keV) than the disks considered in this work.

2.4.4. Comptonization

To calculate the spectrum from inverse Compton scattering through the hot layers of the disk we use a one-dimensional Monte Carlo simulation. The radial variation of quantities in the disk and hot layer is replaced by representative values, for which we use energy-weighted means. The simulation assumes a slab geometry, with the cool optically thick disk below a much hotter surface layer with moderate optical depth. For the seed photons, we use the disk+reflection spectrum found in the previous two sections. To capture the emission lines in this spectrum, we set the resolution of the simulation to $\Delta E/E = 0.046$. The number of seed photons followed through the hot layer is of the order 10^7 , sufficient to represent the re-

sult to a noise level comparable with typical observations. The output spectrum is angle dependent (because of the increasing optical depth with inclination), so a value has to be assumed for the inclination angle θ to the line of sight (measured from the normal of the disk). For our reference model we use $\mu = \cos \theta = 0.5$ as a representative value.

The input parameters of the Comptonization calculation are the input spectrum, the optical depth and the temperature of the hot layer. The resulting total energy flux in Comptonized photons (integrated over the spectrum and summed over both sides of the hot layer) has to match the energy input into the hot layer: the sum of ion heating and viscous dissipation. We can estimate the optical depth for the hot layer from the surface density of the hot layer, where $\langle \tau \rangle = \kappa_{es} \langle \Sigma_{\text{Hot}} \rangle$. The temperature of the hot layer is adjusted iteratively in the calculations to meet this condition to an accuracy of 10%. For the reference model, we find $kT_e = 70$ keV, and $\tau = 0.87$. The resulting emergent spectrum of the hot layer is shown in the blue dotted line in fig. 4, for an inclination angle of $\mu = 0.5$. The photon index of this spectrum in the range 2-10 keV is about $\Gamma = 1.96$.

2.4.5. Treatment of the hot ring

In the hot ring (where the hot layer has spilled over inside inner edge of the cool disk) there is no underlying cool disk any more and it receives its soft photons only by scattering from larger distances: it is 'photon starved' compared with the hot layer itself. Since the energy input by ion heating and viscous dissipation are still similar, the temperature is higher and Comptonization correspondingly stronger. The hot ring therefore makes its contribution mostly at the high energy end of the spectrum, and is less important for the 'soft component' of the spectrum that is the focus of our study. We include it, however, since we also want to achieve a reasonable fit to the overall spectral energy distribution in the observations discussed in the next sections.

The calculation of DS05 relied on the earlier one-dimensional work of Deufel et al. (2002) in order to set the temperature and energetic contribution from the hot inner ring, which predicts a very small contribution from the hot ring. With a sufficiently detailed geometrical model for the hot ring, the soft photon input by scattering could in principle be modelled more accurately, but the level of detail needed is probably beyond the limits of the present model. We therefore treat the soft input flux in this component of the model as an adjustable unknown when fitting to spectra. For this, we introduce a parameter ζ , which represents the fraction of seed photons from the cool disk that cool the hot layer, so that $1 - \zeta$ goes to cool the hot ring. For the reference model, ζ is set by the contribution predicted from the DS05 model for the hot inner ring.

Also treated as adjustable is the temperature reached by equilibrium between heating and Comptonization. We assume that cooling in this region is still moderately efficient, choosing temperatures in the range $kT_e = 180 - 200$ keV. For simplicity (since the angular distribution of seed photons is also uncertain) we model the hot ring with a plane-parallel Monte Carlo simu-

lation with the same resolution as in the hot layer. We discuss the limitations of this approach in sect. 4.

As in the hot layer, the X-ray energy flux produced by Comptonization has to match the energy input by viscous dissipation and ion heating. Together with the now assumed value for the temperature, this determines ζ , and the optical depth of the ring. For the reference parameters of this section, we find $\zeta = 0.99$ and an optical depth of ~ 0.7 . At a temperature of 200 keV we find that the ring contributes only 11% of the overall hard flux ($F_X = 2 - 200$ keV) for the reference values $\alpha = 0.2$ of the viscosity and $R_{in} = 20R_S$.

This is because the radial width of the hot ring has a rather limited extent, since the evaporation process is very efficient. The hot layer evaporates very quickly after it has flowed over inner edge of the cool disk. The hot Comptonized component from the hot ring is shown in the orange dash-dotted line in fig. 4.

2.5. Results for the reference model

The final spectrum and its various components is shown in the top panel of fig 4. The accretion rate for the reference model is $\dot{M}/\dot{M}_{Edd} = 0.002$ assuming an efficiency of 10%, while the luminosity in the 0.5-10 keV range is $L_X/L_{Edd} = 10^{-4}$. The total spectrum is shown in black. The individual components run as follows. The green thermal component (dash-double dotted line) shows the spectral contribution from the outer part of the disk where the hot layer is no longer significant (outside $R/R_S = 100$), while the red long-dashed component shows the rest of the disk and reflection spectrum. For the reference model the reflection ionization parameter is small enough that the reflection and iron line are not apparent in the final spectrum, although we again stress that we are using a reflection model developed for AGN, so in reality the reflection could be stronger. The blue dotted line shows the Comptonized spectrum from the hot layer, while the orange dash-dotted line shows the Comptonized spectrum from the hot ring. Fitting the overall spectrum with a photon index $\Gamma = 1.91$ in the 1-10 keV range, we see a small soft excess below 0.5keV, even though the maximum disk temperature is only 0.05keV. The bottom panel of fig 4 shows the total spectrum divided by a power law with $\Gamma = 1.91$. The observed deviation from a single power law in the hard part of the spectrum (which leads to a deficit around 1 keV and a harder power law index above 10 keV) is caused by anisotropic Comptonization resulting from considering a plane-parallel configuration (see e.g. Haardt (1993) and sect. 4 of this paper), and also by the contribution from the hot ring. Except for the very low accretion rate, we see a spectrum that is qualitatively similar to those of Miller et al. (2006a) and Miller et al. (2006b).

3. Comparison to observations

The luminosity of our reference model described above, of the order $10^{-4}L_{Edd}$ is substantially lower than the luminosities (of the order 3×10^{-2} - $10^{-3}L_{Edd}$) inferred for the observed sources to which we want to apply the model. This is a consequence of the flow model in DS05 that is the basis of our analysis. In it,

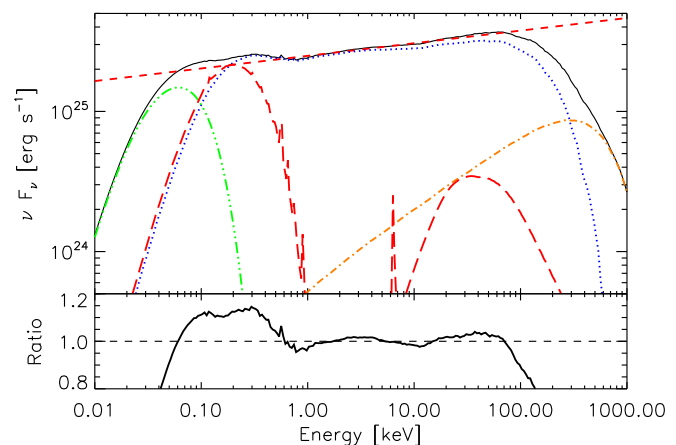


Fig. 4. Top: Relative contribution from each component for reference model, $\alpha = 0.2$, $R_{in} = 20R_S$, $M = 10M_\odot$. Red long-dashed line: Spectrum from the disk (modified blackbody plus reflection spectrum). Green dash-double dotted line: Spectrum from outer disk. Blue dotted line: Comptonized spectrum from hot layer. Orange dash-dotted line: Comptonized spectrum from hot ring. Black: total spectrum. Red short-dashed: power law with $\Gamma = 1.9$. Bottom: Total spectrum divided by power law with $\Gamma = 1.9$.

the surface density of the hot layer is governed by the physics of the Coulomb interaction of the hot ions penetrating through it, and its temperature by the energy balance between it and the underlying disk. With temperature and surface density constrained in this way, the mass flux then depends only on the radial drift speed, i.e. the viscosity parameter, α . The actual mass flux is low because the temperature of the layer is only about 80keV. This suggests that the current model is incomplete, and we discuss a possible solution in sect. 4. In this paper, however, we solve this problem by introducing a parameter, C , by which the accretion rate (or equivalently the energy output of each component of the flow) is increased. This makes the implicit assumption that increasing the accretion rate causes the energy output in each component to increase, but the relative contribution of each component to the overall energy budget and geometric configuration of the flow to stay constant. Scaling the accretion rate in this way increases the luminosity in all components, which thus causes an increase in temperature for the cool disk at a fixed truncation radius.

With the introduction of the parameters C and ζ our model loses its predictive power, but the goal of this paper is to present a model that is plausible rather than precise in its details. In the next section we compare our spectra to the best fits from observations, and show that for reasonable values of the hot layer and inner ring and accretion rate, we can reproduce the observed soft excesses using a significantly truncated accretion disk.

To illustrate how our model can be made consistent with observed soft excesses, we perform a qualitative comparison between the soft excesses observed in SWIFT J1753.5-0127 (Miller et al. 2006a) and GX 339-4 (Miller et al. 2006b) and our model. For each object we use the estimates for black hole

mass, inclination and distance to source presented in those two papers and take $\alpha = 0.2$ as a standard value for the viscosity parameter. We then assume a moderate truncation radius and find a solution for energy and surface density as was discussed in sect. 2, and calculate the spectrum. We change C (the accretion rate) and ζ (the ratio between seed photons in the hot layer and inner ring) in order to match the luminosity and spectral index of the best fit to the observed spectrum, and compare our soft excess to the observed one. If necessary we also change the amount of interstellar absorption, although for both the cases we consider we do not need to change it very much. Given the systematic uncertainties in our model, a more statistical comparison to the data is not possible; our goal is instead to demonstrate that we are able to reproduce the observed spectra with physically reasonable parameters.

3.1. SWIFT J1753.5-0127

We begin with the spectrum from the source SWIFT J1753.5-0127. Miller et al. (2006a) took a 42 ksec *XMM-Newton* observation and estimated an X-ray luminosity (0.5-10 keV) of $L_X/L_{\text{Edd}} = 2.6 \times 10^{-3} (d/8.5 \text{ kpc})^2 (M/10 M_\odot)$. They fit the spectrum to a power law with a photon index $\Gamma = 1.67$ (2-10 keV), and interstellar absorption of $N_{\text{H}} = 2.3 \times 10^{21} \text{ cm}^{-2}$. Fitting the spectrum with an absorbed power law component alone reveals a small soft excess below 2 keV, which they fit to a disk with $kT_{\text{in}} \approx 0.22 \text{ keV}$ and $R_{\text{in}} \approx R_{\text{S}} (M/10 M_\odot) (d/8.5 \text{ kpc}) / \cos^{1/2} i$.

A very truncated disk will be too cool to be observable in X-rays, while an untruncated disk will have a higher temperature than is observed (because of the effects of heating from the corona). To compare with the observed spectra we assume a moderate truncation radius of $15R_{\text{S}}$, which is qualitatively very different from an untruncated disk (which will have an inner radius between $0.5 - 3R_{\text{S}}$ depending on the spin of the black hole). We make the same assumptions for mass ($M = 10M_\odot$) and distance ($d = 8.5 \text{ kpc}$) as in Miller et al. (2006a) and assume an inclination of $\mu = 0.5$. The simulation then predicts an accretion rate of $\dot{M}/\dot{M}_{\text{Edd}} = 1.5 \times 10^{-3}$ for an efficiency of 10%. In order to match the measured flux in the power law component, we increase the flux in each component by a factor $C = 12$, to give an accretion rate $\dot{M}/\dot{M}_{\text{Edd}} = 1.7 \times 10^{-2}$.

In the hot layer, the predicted surface density profile gives the optical depth $\langle \tau \rangle = 0.87$, and the energy balance between the cool disk and hot layer (see sect. 2.3) determines a temperature of $kT_e = 75 \text{ keV}$, which gives a photon index of $\Gamma = 1.87$ (3-10 keV).⁴ The density of the disk and flux in the hot layer also allows us to estimate the ionization parameter, $\xi = 50 \text{ erg cm s}^{-1}$, from which we get an albedo and find that the Comptonized flux incident on the disk heats it to $kT_e = 0.11 \text{ keV}$, which looks like $kT_e = 0.19 \text{ keV}$ when spectral hardening is taken into account.

⁴ The spectral index of a Comptonizing corona will change depending on viewing angle, since the mean optical depth will change depending on whether the disk is face-on or tilted, which will harden the spectrum. To calculate the energy in the hot layer and thus its temperature we take the spectral index for the spectrum integrated from 0° - 180° .

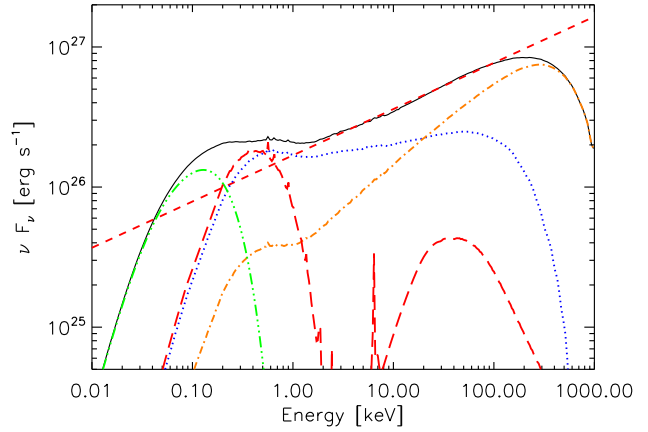


Fig. 5. Model spectrum for SWIFT J1753.5-0127, for a truncated disk with inner radius of $15 R_{\text{S}}$ with $\alpha = 0.2$ and $M = 10M_\odot$. Red long-dashed line: Spectrum from the disk (modified blackbody plus reflection spectrum). Green dash-double dotted line: Spectrum from outer disk. Blue dotted line: Comptonized spectrum from hot layer. Orange dash-dotted line: Comptonized spectrum from hot ring. Black: total spectrum. Red short-dashed: power law with $\Gamma = 1.66$.

The predicted surface density in the hot inner ring also allows us to calculate the optical depth of this layer, which we find to be $\langle \tau \rangle = 0.7$. Since we do not have a detailed model for the radiative transfer in this component, we take a plausible value of $kT = 200 \text{ keV}$, which gives a photon index of $\Gamma = 1.39$ between 2 and 10 keV. The resulting spectrum is still too soft, so we set $\zeta = 0.89$, meaning that 89% of the disk and reflection photons are used to seed the hot layer, while the rest seed the hot inner ring. Figure 5 shows the resulting spectral energy distribution for SWIFT J1753.5-0127. The different components shown in the figure are the same as in fig. 4.

Figure 6 (taken from Miller et al. (2006a)) shows the spectrum divided by an absorbed power law with an absorption column density of $N_{\text{H}} = 2.3 \times 10^{21} \text{ cm}^{-2}$. Overlaid we show their best fit using the XSPEC “diskbb+pow” model (in red) and the soft excess predicted by our model (in green). To obtain a better fit we change the absorption column density to $N_{\text{H}} = 2.35 \times 10^{21} \text{ cm}^{-2}$ to render the two excesses effectively indistinguishable, even though the temperature and peak fluxes of both disks are very different. We discuss the reasons for this at the beginning of sect. 4.3. Figure 6 also shows that the deviation from a simple power law in the range 2-100 keV is less than 10%, which is consistent with observation.

3.2. GX 339-4

Our second source for comparison is the relatively better constrained X-ray source GX 339-4. This source has an estimated mass of $6M_\odot$, distance of around 8 kpc and inclination $\mu = 0.9$. Miller et al. (2006b) took a 280ks *XMM-Newton* observation of this source, which they observed at a flux of about $L_X/L_{\text{Edd}} \approx 0.05 (M/10M_\odot) (D/8 \text{ kpc})$. They fit the data with a moderate ab-

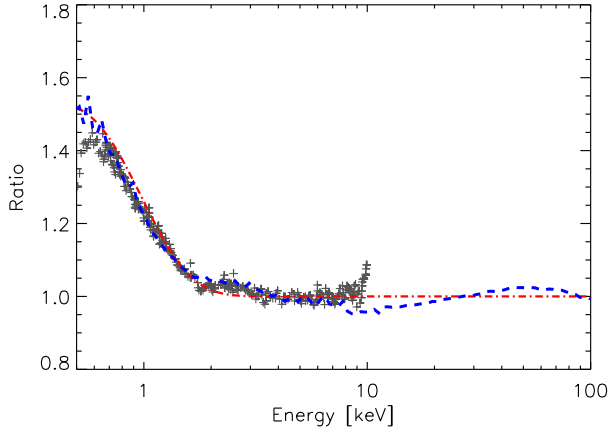


Fig. 6. The soft excess in SWIFT J1753.5-0127. The crosses show the observed spectrum divided by a simple power law fit above 3 keV with a best-fit column density of $N_{\text{H}} = 2.3 \times 10^{21} \text{ cm}^{-2}$, taken from fig. 2 of Miller et al. (2006a). The dashed-dotted red line shows the best fit two-component XSPEC “diskbb+pow” divided by the same power law (as reported in Miller et al. (2006a)). The dashed blue line shows the ratio between our best fit model (see fig. 5) and the same power law, with an increase of $0.05 \times 10^{21} \text{ cm}^{-2}$ in interstellar absorption.

sorption column density ($N_{\text{H}} = 3.72 \times 10^{21} \text{ cm}^{-2}$) and very hard power law ($\Gamma = 1.44$) and find a soft excess below 3 keV which they fit to a disk with $R_{\text{in}} = 0.6R_{\text{S}}$ and $kT_{\text{in}} = 0.38$ keV. Additionally, they observe a broad asymmetric Fe-K line with a maximum at 6.9 keV, from which they measure a reflection fraction of about 0.2-0.3 and ionization parameter $\xi \sim 10^3$ erg cm s $^{-1}$. Fitting the Fe-K line using relativistic broadening suggests an inner radius of $0.7R_{\text{S}}$.

For an assumed radius of the inner edge of the disk $R_{\text{in}} = 19R_{\text{S}}$, a good fit for this source is obtained with the following set of parameter values: $C=77$ (or $\dot{M}/\dot{M}_{\text{Edd}} = 0.15$), $\zeta=0.63$, and the temperature of the hot layer and hot ring 75 keV, and 200 keV respectively. The resulting spectral energy distribution is shown in fig. 7. Figure 8 shows the soft excess observed in Miller et al. (2006b). The luminosity enhancement factor is higher than for the SWIFT source because of the higher luminosity inferred from the observations. The ionization parameter in the reflection region is also higher, with $\xi = 550$ erg cm s $^{-1}$.

Note the structure in the data around 1 keV, which is suggestive of the structure of the interstellar absorption in this region of the spectrum. In fact, we can best reproduce the observation for a column $N_{\text{H}} = 4.9 \times 10^{21} \text{ cm}^{-2}$, some 30% higher than found by Miller et al. (2006b).

As is seen in fig. 8, we also find an Fe-K emission line in our fit, with a strength comparable to the observations. The combination of parameters that fits the overall spectral shape in our model therefore also fits the reflection component of the spectrum. Since this component depends on details of the interaction between the hot layer and the cool disk under it, this adds some confidence in this part of the physics of our model.

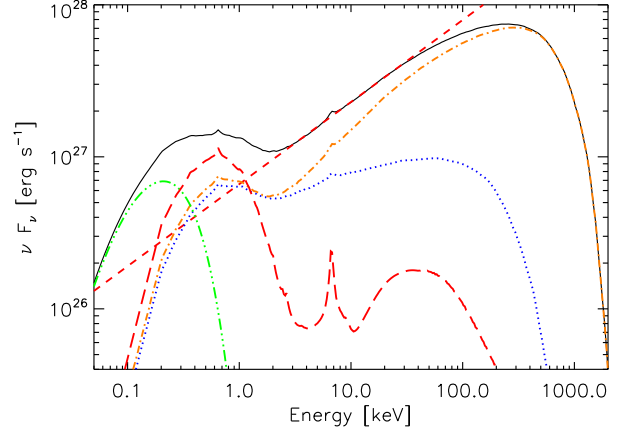


Fig. 7. Model spectrum for GX339-4, for a truncated disk with an inner radius of $19R_{\text{S}}$, $\alpha = 0.2$ and $M = 6M_{\odot}$. Red long-dashed line: Spectrum from the disk (modified blackbody plus reflection spectrum). Green dash-double dotted line: Spectrum from outer disk. Blue dotted line: Comptonized spectrum from hot layer. Orange dash-dotted line: Comptonized spectrum from hot ring. Black: total spectrum. Red short-dashed: power law with $\Gamma = 1.47$.

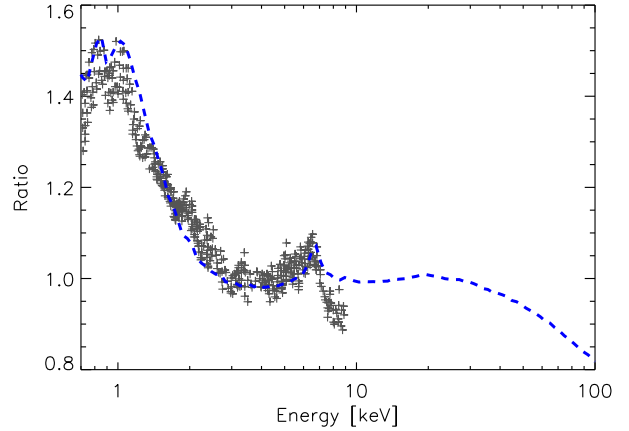


Fig. 8. The soft excess in GX 339-4, taken from fig. 3 of Miller et al. (2006b). The crosses show the spectrum divided by a simple power law fit to the *XMM-Newton* and *RXTE* spectra with an absorption column density of $N_{\text{H}} = 3.72 \times 10^{21} \text{ cm}^{-2}$. The 4-7 keV range, where a broad Fe-K line is clearly visible, was omitted from the fit. The dashed blue line shows the ratio between our best fit model (see fig. 7) and the same power law fit with interstellar absorption $N_{\text{H}} = 4.9 \times 10^{21} \text{ cm}^{-2}$.

4. Discussion

In the paper thus far we have produced spectra of an ion-bombardment model with a truncated disk for Low-Hard state accretion, incorporating a spectrally-hardened blackbody component, physical reflection models from the literature and a Monte Carlo Comptonization calculation.

Detailed fits to observations have shown that the model can reproduce the observed soft excess, high-energy spectral index

and the approximate strength of the Fe-K line in GX 339-4. We have also shown that the structure observed in the soft excess in GX 339-4 is consistent with interstellar absorption features, suggesting that the absorption column density for this source might be underestimated.

However, we have also found that further work is necessary to develop the flow model outlined in Deufel et al. (2002) and DS05. Most significantly, a large viscosity in the hot regions of the flow (the hot layer and ADAF) is required to increase the accretion rate sufficiently to match observations. This may suggest the presence of strong ordered magnetic fields in the inner regions of the accretion flow, which are also believed to be associated with observed jets.

4.1. Mass flux in the hot layer

As was discussed in sect. 3, the global accretion rate in the present model is limited by the rate at which the hot layer can flow over the cool disk. The surface density and temperature of the hot layer are in turn narrowly constrained by the physics of the Coulomb interaction which allow the layer to form and the energy balance between it and the underlying disk. There are thus two ways to increase the flow rate in the hot layer: by increasing the effective viscosity or providing another mechanism besides viscous dissipation to transport angular momentum.

The interaction between the ion supported ADAF and the hot layer provides such a mechanism. The ion supported flow is partially supported against gravity by gas pressure and rotates slower than Keplerian. The mass condensing from the ADAF on the hot layer thus acts as a sink of angular momentum, which increases the mass flux in the hot layer. This effect was not included in DS05 and the calculations above. An estimate of its importance can be made by evaluating the angular momentum exchange *a posteriori* from the solutions in sect. 3. We find that, for the viscosity parameter $\alpha = 0.2$ assumed for the hot layer, the effect increases the mass flux by a factor 2–3. The effect is thus significant, but not sufficient to increase the mass flux by the factors indicated by the comparison with observations in sect. 3.

The missing ingredient most likely to lead to the higher mass fluxes inferred from the observations may well be a strong magnetic field. Strong ordered magnetic fields in the inner regions of the flow are implied by the presence of jets, especially in the hard X-ray states discussed here. A bundle of strong ordered magnetic field held together by a disk (Bisnovatyi-Kogan & Ruzmaikin 1974) can have field strengths well above those produced by magnetorotational turbulence. The angular momentum exchange by interaction of such a bundle with the disk (Stehle & Spruit 2001; Igumenshchev et al. 2003; Narayan et al. 2003; De Villiers et al. 2005) can be much more effective than turbulence parametrized with a viscosity parameter $\alpha \sim 1$. This aspect is beyond the present study, and is a promising field for further study.

4.2. Spectrum of the hot ring

The spectrum from the hot ring in our model is hard to predict without a more detailed model. The uncertainty lies chiefly in the distribution and number of seed photons available for cooling. The more photon-starved the hot ring is, the higher its temperature will be, and (since the evaporation rate into an ADAF scales with T_e^2) the smaller its contribution to the overall spectrum. The temperature we assumed for the hot ring in practice could be much lower, which would bring it more in line with observations of the high energy cutoff observed in some spectra (which suggest a maximum temperature of about $kT_e \sim 150$ keV). Additionally, the geometric distribution of seed photons will change the structure of the Compton spectrum. This is because photons that scatter once preferentially scatter back in the direction they were originally travelling, and there is a deficit of photons in the first scattering hump in the spectrum. This effect is most pronounced in the plane-parallel case (e.g. Haardt & Maraschi (1991)), but there will also be some anisotropy in the hot ring's spectrum if the seed photons are primarily from the disk. We have considered only seed photons from the disk, but there may also be photons produced from other processes (such as synchrotron emission) which would allow the hot ring to cool more efficiently and make the effects of anisotropy less pronounced (since the seed photons would be travelling through the hot ring in essentially random directions). Finally, in this paper we have neglected the spectral contribution from the ADAF. Depending on its radiative efficiency, its contribution could also harden the observed high-energy Comptonized spectrum considerably.

4.3. Comparison with other work

Our model of a disk truncated at 15–20 R_S and surrounding corona is qualitatively very different from the untruncated disk (with $R_{in} \sim 1R_S$) models fit by Miller et al. (2006a) and Miller et al. (2006b), and it is natural to ask how the observed soft excess can be so small when the radiating area is so much larger. The answer lies in several points. The most important of these is that the temperature in our disks is about a factor 2 smaller than is found by Miller et al. (2006a), so that the flux is intrinsically much smaller and (even after the colour-correction is applied) most of the flux is cut off by interstellar absorption. There is a further reduction from the hot surface layer, which upscatters about two-thirds of the photons. Finally, the shape of the upscattered photons deviates from a power law at low energies, so that measuring the temperature of the soft excess depends very sensitively on modelling the Comptonized spectrum correctly.

The effects of irradiation on the measured truncation radius have also been studied using a more phenomenological approach in Gierliński et al. (2008), who re-analyzed the data from J1817-330 (Rykoff et al. 2007) to demonstrate that irradiation can increase the measured truncation radius in this source (although they assume continual stress at the inner boundary of the truncated disk, which we have not done here). In particular, they note future plans to test the effects of incomplete

thermalization from incident radiation (cf. sect. 2.4.1), which can further increase the truncation radius.

Several well-studied sources show some evidence of deviations from a single power law. Done et al. (2007) notes that spectra from Cyg X-1 have additional structure in their spectra that can be fit with an additional very soft Comptonizing component, while both the source GX 339-4 and Cyg X-1 sometimes show an excess of very high energy photons compared to a fit with a single power law, which suggests a second site for Comptonization that is naturally explained with this model.

For GX 339-4, Miller et al. (2006b) detected a broad Fe-K line, which they fitted with a relativistically broadened profile, implying an untruncated disk and a spinning black hole. However, the observation of a broadened Fe-K line may also be consistent with a truncated disk if the broadening instead comes from an outflow, as has been suggested in Done & Gierliński (2006) and Laurent & Titarchuk (2007).

The truncated disk picture of hard states in X-ray binaries has received support from analyses of the noise spectrum of the X-ray variability. In the model by Churazov et al. (2001), for example, the characteristic frequency at ~ 0.01 Hz in Cyg X-1 corresponds to the viscous frequency ($\sim v_r/r$) of a geometrically thin accretion flow at a truncation radius of about $25R_S$. X-ray timing data typically contain several characteristic frequencies, while theoretical models allow for different mechanisms of variability (eg. Giannios & Spruit (2004)). The model presented here does not contain enough physics to make predictions about the source and nature of X-ray variability. For reference we note that, for a truncation radius at $20R_S$, the viscous frequencies for our model are ~ 0.8 Hz for the hot layer, ~ 2 Hz for the hot ring, and ~ 50 Hz for the ADAF. 1 Hz is a characteristic frequency often observed in Cyg X-1.

The physics of interaction of an ion-supported flow with a cool disk is very well defined. The process produces a hot layer of tightly constrained thickness and temperature. The physics is detailed enough, for example, to be implemented in a numerical hydrodynamic simulations of the accretion flow. The present model falls short of achieving this: the inner hot ring where the evaporation into the ADAF takes place, in particular, contains parametrizations that would need to be improved with a more detailed (2-D) treatment of radiative transfer. Thus the model used here has adjustable parameters but compared with other hot corona models there is a straightforward path to more rigorous calculations.

Note, however, that the likely presence of a strong ordered magnetic field in the inner regions of the accretion (see 4.1 and 4.2 above) adds additional physics that is not included either in existing hot corona models or the present ion illumination model.

5. Conclusions

From energetic considerations, the hard spectra observed in the low-hard state of LMXBs must be produced by hot ($kT_e \sim 100$ keV) matter in the inner regions surrounding the black hole. If there is also a much cooler disk present, there will necessarily be some degree of interaction between the two components, and the disk will be somewhat heated by irradiation from the

hot Comptonizing component. The fits reported in Miller et al. (2006a) and Miller et al. (2006b) neglect this interaction by fitting the disk and hard component separately. In this paper we have shown that incorporating the effects of this interaction heats the inner regions of a moderately truncated disk so that, when coupled with the effects of interstellar absorption, the size of the soft excess matches observations. Our work also highlights the potential pitfalls of using simple power law or analytic Comptonization fits at low energies, which can provide significant deviations in the soft X-rays, thus changing the shape and intensity of the observed soft excess.

In the case of GX 339-4, our model predicts an Fe-K component of comparable strength to that observed, although we did not do a detailed comparison. However, work by others has suggested that part of the broadening in the Fe-K line that was observed for GX 339-4 can be attributed to a large outflow, and detailed models of Fe-K fluorescence in galactic black holes show lines that are much broader than is found in AGN models (and which are normally used to fit spectra).

The model we have envisioned presents several opportunities for further improvement, in order to better constrain the introduced fitting parameters, C and η . The spectrum from the hot ring and ADAF are particularly uncertain, and dependent on a more detailed model for the radiative transfer through this region, as well as the source and number of seed photons (which will set the electron temperature in both regions). The model's global accretion rate (which is limited by the rate at which the hot layer spills over into the hot ring and then evaporates into the ADAF) is also very low, although this can be increased if the viscosity in the warm layer can be increased, perhaps as a result of accretion through an ordered magnetic field.

CD'A acknowledges financial support from the National Sciences and Engineering Research Council of Canada.

References

- Ballantyne, D. R., Ross, R. R., & Fabian, A. C. 2001, MNRAS, 327, 10
- Balucinska-Church, M., Belloni, T., Church, M. J., & Hasinger, G. 1995, A&A, 302, L5+
- Beloborodov, A. M. 1999, ApJ, 510, L123
- Bisnovatyi-Kogan, G. S. & Ruzmaikin, A. A. 1974, Ap&SS, 28, 45
- Brockopp, C., McGowan, K. E., Krimm, H., et al. 2006, MNRAS, 365, 1203
- Churazov, E., Gilfanov, M., & Revnivtsev, M. 2001, MNRAS, 321, 759
- Davis, S. W., Blaes, O. M., Hubeny, I., & Turner, N. J. 2005, ApJ, 621, 372
- De Villiers, J.-P., Hawley, J. F., Krolik, J. H., & Hirose, S. 2005, ApJ, 620, 878
- Deufel, B., Dullemond, C. P., & Spruit, H. C. 2002, A&A, 387, 907
- Deufel, B. & Spruit, H. C. 2000, A&A, 362, 1
- di Matteo, T. 1998, MNRAS, 299, L15+
- Di Salvo, T., Done, C., Życki, P. T., Burderi, L., & Robba, N. R. 2001, ApJ, 547, 1024
- Done, C. & Gierliński, M. 2006, MNRAS, 367, 659

- Done, C., Gierliński, M., & Kubota, A. 2007, *A&A Rev.*, 15, 1
- Dullemond, C. P. & Spruit, H. C. 2005, *A&A*, 434, 415
- Esin, A. A., McClintock, J. E., & Narayan, R. 1997, *ApJ*, 489, 865
- Giannios, D. & Spruit, H. C. 2004, *A&A*, 427, 251
- Gierliński, M., Done, C., & Page, K. 2008, *MNRAS*, 717
- Haardt, F. 1993, *ApJ*, 413, 680
- Haardt, F. & Maraschi, L. 1991, *ApJ*, 380, L51
- Igumenshchev, I. V., Narayan, R., & Abramowicz, M. A. 2003, *ApJ*, 592, 1042
- Laurent, P. & Titarchuk, L. 2007, *ApJ*, 656, 1056
- Merloni, A. & Fabian, A. C. 2001, *MNRAS*, 321, 549
- Merloni, A., Fabian, A. C., & Ross, R. R. 2000, *MNRAS*, 313, 193
- Miller, J. M., Homan, J., & Miniutti, G. 2006a, *ApJ*, 652, L113
- Miller, J. M., Homan, J., Steeghs, D., et al. 2006b, *ApJ*, 653, 525
- Narayan, R., Igumenshchev, I. V., & Abramowicz, M. A. 2003, *PASJ*, 55, L69
- Narayan, R. & Yi, I. 1994, *ApJ*, 428, L13
- Nayakshin, S. & Kallman, T. R. 2001, *ApJ*, 546, 406
- Nayakshin, S., Kazanas, D., & Kallman, T. R. 2000, *ApJ*, 537, 833
- Ramadevi, M. C. & Seetha, S. 2007, *MNRAS*, 378, 182
- Ross, R. R. & Fabian, A. C. 2005, *MNRAS*, 358, 211
- Ross, R. R. & Fabian, A. C. 2007, *MNRAS*, 381, 1697
- Rykoff, E. S., Miller, J. M., Steeghs, D., & Torres, M. A. P. 2007, *ApJ*, 666, 1129
- Shakura, N. I. & Sunyaev, R. A. 1973, *A&A*, 24, 337
- Shimura, T. & Takahara, F. 1995, *ApJ*, 445, 780
- Spruit, H. C. 1997, in *LNP Vol. 487: Accretion Disks - New Aspects*, ed. E. Meyer-Hofmeister & H. Spruit, 67–76
- Spruit, H. C. & Deufel, B. 2002, *A&A*, 387, 918
- Stehle, R. & Spruit, H. C. 2001, *MNRAS*, 323, 587
- Taam, R. E., Liu, B. F., Meyer, F., & Meyer-Hofmeister, E. 2008, *ArXiv e-prints*, 807
- Takahashi, H., Fukazawa, Y., Mizuno, T., et al. 2008, *PASJ*, 60, 69
- Tomsick, J. A., Kalemci, E., Kaaret, P., et al. 2008, *ArXiv e-prints*, 802